Published in final edited form as:
Microbiol Res. 2011 October 20; 166(7): 521–530. doi:10.1016/j.micres.2010.10.004.

^{13}C–Metabolic enrichment of glutamate in glutamate dehydrogenase mutants of *Saccharomyces cerevisiae*

Yijin Tang, **Alex Sieg**, and **Pamela J. Trotter***
Guehler Biochemistry Laboratory, Department of Chemistry, Augustana College, 639-38thStreet, Rock Island, IL 61201

Abstract

Glutamate dehydrogenases (GDH) interconvert α-ketoglutarate and glutamate. In yeast, NADP-dependent enzymes, encoded by *GDH1* and *GDH3*, are reported to synthesize glutamate from α-ketoglutarate, while an NAD-dependent enzyme, encoded by *GDH2*, catalyzes the reverse. Cells were grown in acetate/raffinose (YNAceRaf) to examine the role(s) of these enzymes during aerobic metabolism. In YNAceRaf the doubling time of wild type, *gdh2Δ*, and *gdh3Δ* cells was comparable at ~ 4 hours. NADP-dependent GDH activity (Gdh1p + Gdh3p) in wild type, *gdh2Δ*, and *gdh3Δ* was decreased ~80% and NAD-dependent activity (Gdh2p) in wild type and *gdh3Δ* was increased ~20-fold in YNAceRaf as compared to glucose. Cells carrying the *gdh1Δ* allele did not divide in YNAceRaf, yet both the NADP-dependent (Gdh3p) and NAD-dependent (Gdh2p) GDH activity was ~3-fold higher than in glucose. Metabolism of [1, 2-^{13}C]-acetate and analysis of carbon NMR spectra was used to examine glutamate metabolism. Incorporation of ^{13}C into glutamate was nearly undetectable in *gdh1Δ* cells, reflecting a GDH activity at < 15% of wild type. Analysis of ^{13}C- enrichment of glutamate carbons indicate a decreased rate of glutamate biosynthesis from acetate in *gdh2Δ* and *gdh3Δ* strains as compared to wild type. Further, the relative complexity of ^{13}C-isotopomers at early time points was noticeably greater in *gdh3Δ* as compared to wild type and *gdh2Δ* cells. These *in vivo* data show that Gdh1p is the primary GDH enzyme and Gdh2p and Gdh3p play evident roles during aerobic glutamate metabolism.

Introduction

The yeast *Saccharomyces cerevisiae* thrives with ammonia as its only source of nitrogen, as it is capable of assimilating ammonia into glutamate, which accounts for about 80% of cellular nitrogen (Magasanik, 2003). Glutamate may be produced in two ways. An ATP-dependent glutamine synthetase (encoded by *GLN1*) may catalyze the transfer of ammonia onto glutamate, producing glutamine. This is followed by the action of a NAD-dependent glutamate synthase (encoded by *GLT1*), which reduces and transfers the amide group onto α-ketoglutarate (2-oxoglutarate) to produce two molecules of glutamate. Alternatively, in the favored route at lower metabolic cost, two NADP-dependent glutamate dehydrogenases (NADP-GDH; encoded by *GDH1* and *GDH3*) produce glutamate by catalyzing amination and reduction of α-ketoglutarate (Magasanik, 2003; DeLuna et al, 2001). Degradation of glutamate to α-ketoglutarate and free ammonia is mediated by a related NAD-dependent glutamate dehydrogenase (NAD-GDH; encoded by *GDH2*) (Miller and Magasanik, 1990).

*Corresponding author: pamtrotter@augustana.edu.

Studies by DeLuna *et al.* (2001) on the expression and activity levels of the three glutamate dehydrogenase enzymes indicate that Gdh1p is the sole NADP-GDH showing activity when cells grow on glucose. Gdh3p is induced during the diauxic shift or by growth in ethanol, indicating a role during respiration, whereas Gdh1p activity is the same or decreased under these conditions. The Gdh2p enzyme is also subject to regulation (Coschigano et al, 1991), being repressed by glucose and elevated during fermentation (low glucose, ethanol), respiration (acetate) or growth with amino acids as nitrogen source. Such control is consistent with an anapleurotic role for Gdh2p during respiration (Coschigano et al, 1991).

The regulation of the GDH enzymes indicates different physiological roles in the cell. In these studies we aimed to examine the biosynthesis of glutamate *in vivo* using ^{13}C-metabolic enrichment followed by nuclear magnetic resonance (NMR) spectral analysis. Glutamate formation was examined during aerobic metabolism in normal, wild type cells as compared to single disruption mutants for each of the GDH enzymes (*gdh1Δ*, *gdh2Δ* and *gdh3Δ*). These data allow us to make some conclusions about the relative importance of each of the three enzymes in regulating the level of glutamate formation during aerobic metabolism.

Materials and Methods

Yeast strains, media and growth

The yeast strains used in these studies and their genotypes are listed in Table I. Genotypes were confirmed by growth phenotype for nutritional markers or PCR analysis of *GDH* alleles (data not shown). Synthetic medium (YN) contained 0.6% yeast nitrogen base, 0.5% yeast extract, and the necessary amino acid supplements, see Table 1 (Sherman, 1991). The carbon sources were either 2% glucose (YNDex) or 1% each of acetate and raffinose (YNAceRaf). Minimal medium for ^{13}C-metabolic enrichment contained 0.67% yeast nitrogen base without amino acids. All media reagents were from Difco or Sigma Chemical.

Doubling times were determined for cells during logarithmic growth. YNDex-grown cells were diluted to an optical density of 0.05–0.2 at 600 nm (OD_{600}) and OD_{600} readings were taken for 8 (YNDex) to 24 (YNAceRaf) hours at 30 C with shaking at 200rpm. Growth after the transfer of cells from YNDex to YNAceRaf proceeded only after a significant lag (~10 hours; data not shown). To examine the viability of *gdh1Δ* cells after culture in YNAceRaf medium, cells pre-grown overnight in YNDex were pelleted by centrifugation, resuspended in YNAceRaf, and cultured for an additional 17–19 hours. The number of live cells in the culture was determined before and after incubation in YNAceRaf by spreading a dilution of cells onto duplicate rich YPD plates (Sherman, 1991) and counting the number of resulting colonies.

Growth conditions used for enzyme determination and metabolic enrichment were essentially the same as those above. For glucose grown cells, cell lysates were prepared from late log phase cells grown overnight in YNDex. For cells grown in YNAceRaf, cells were first grown up overnight in YNDex. Cells were then pelleted by centrifugation, resuspended in fresh YNAceRaf medium, and allowed to grow to late log phase (16–18 hours) with shaking at 30°C.

Glutamate dehydrogenase assays

Cell lysates were prepared by glass bead disruption in 0.1M potassium phosphate, pH 7.8 as described previously (Trotter et al, 2005). Aliquots were stored at −20°C and thawed on the day of the assay. Glutamate dehydrogenase activity was measured by monitoring the oxidation of NADPH or NADH spectrophotometrically by the method of Doherty (1970). Protein concentrations were determined by BCA (bicinchoninic acid) assay (Sigma Chemical).

NMR studies

Cells were washed with sterile diH_2O and pellets were resuspended (0.5–0.75 g) in minimal medium containing 0.5 mg/mL of [1,2-^{13}C]-acetate (Cambridge Isotope Labs). Cells were incubated with shaking at 30°C for the time indicated. Following incubation, cell extracts were prepared as described previously (Trotter et al, 2005) with one modification. The extracts were dried overnight with a Jouan RC1010 vacuum centrifuge and the dried extract was dissolved in deuterated water (D_2O; Cambridge Isotope Labs). NMR spectroscopy was performed on a JEOL ECA-400 MHz instrument. Proton-decoupled ^{13}C NMR spectra were obtained at 100.6 MHz using WALTZ-16 proton decoupling, a 45° pulse width, 5s delay, 20,000-Hz sweep width, and 32,000 data points. The number of scans per sample was set at 4096.

Delta software (JEOL) was used for spectral processing. Glutamate peaks were identified based upon published shift values, shift values observed using standards, and our previous studies (Trotter et al, 2005). Carbon-13 enrichment with the acetate precursor resulted in glutamate signals appearing as multiplets, rather than the singlets seen in molecules with natural abundance of ^{13}C. Relative total, singlet, doublet, and/or multiplet ^{13}C signal intensities for the carbons of glutamate were determined by integration as previously described (Trotter et al, 2005).

Results

Characteristics of strains under experimental conditions

Culture conditions were chosen such that all three GDH enzymes might be measurably active - *i.e.* in the absence of glucose - and the mutant strains might have the best growth performance. The trisaccharide raffinose was chosen as one carbon source because it allows for de-repression of glucose repressed genes, while still supporting growth of some yeast strains carrying mitochondrial deficiencies (Reilly and Sherman, 1965; Zitomer and Nichols, 1978). Acetate was also included to allow cells to adapt to this carbon source (De Virgilio et al, 1992; van den Berg et al, 1996; Tenreiro et al, 2000) prior to metabolic enrichment with the isotope-labeled form. Thus, experiments were conducted with cells grown either in 2% glucose (YNDex) or a mixture of 1% acetate and 1% raffinose (YNAceRaf) and containing ammonia as the primary nitrogen source. The doubling times of the strains in both media are shown in Table I. With the exception of *gdh1Δ* in YNAceRaf, the strains have comparable doubling times in either medium. Although the *gdh1Δ* cells do not double in YNAceRaf, cell viability is unaffected after 17–19 hours culture in this medium (see Materials and Methods, data not shown).

NAD(P)-dependent GDH activity was measured in extracts from cells grown in either medium. Total NADP-dependent GDH activity (primarily Gdh1p) in the wild type, *gdh2Δ*, and *gdh3Δ* strains is decreased in YNAceRaf as compared to YNDex (Table 2, left). Yet, the small amount of NADP-dependent activity in *gdh1Δ* cells (presumably due to Gdh3p) increases; this suggests that, although NADP-dependent GDH overall is decreased, the proportion of NADP-dependent activity due to Gdh3p is higher in YNAceRaf medium. NAD-dependent Gdh2p activity is significantly elevated in cells grown on YNAceRaf as compared to YNDex (Table 2, right). This is true even in the non-dividing, *gdh1Δ* cells. Collectively, these data indicate that all of the NADP- and NAD-dependent GDH enzyme activities are present at measureable levels in cells grown in YNAceRaf medium.

Metabolic enrichment studies

Metabolic enrichment with ^{13}C precursor was used to examine glutamate metabolism, as the observed characteristics of NMR spectra can provide information about the movement of

carbons through the pathway(s). The abundance of ^{13}C in nature is such that, without enrichment, each of the carbons in glutamate appears as a single resonance in a proton-decoupled ^{13}C spectrum. With metabolic enrichment, the introduced ^{13}C-label stands out above the natural signal (not shown). During metabolic incorporation of [1, 2-^{13}C]-acetate, the ratio of ^{13}C signal in carbon 2 (C2) compared to carbon 4 (C4) of glutamate reflects the relative rate of incorporation of [1,2-^{13}C]-acetate. The schematic in Figure 1 depicts [1,2-^{13}C]-acetate incorporation, which forms ^{13}C-isotopomers of glutamate with consecutive rotations of the citric acid cycle. Increasing enrichment of ^{13}C relative to ^{12}C at each position is represented by darker shading. Note that ^{13}C enrichment of glutamate C4 precedes that of C2. Increasing ^{13}C enrichment of neighboring carbons is responsible for characteristic splitting of carbon resonances observed in NMR spectra (Jeffrey et al, 1991;Burgess et al, 2001;Trotter et al, 2005).

Cells were pre-grown in YNAceRaf medium, incubated with [1, 2-^{13}C]-acetate in minimal medium for a desired time, and extracts prepared for NMR analysis. Proton-decoupled ^{13}C NMR spectra were obtained and glutamate peaks were identified based upon known shift values. The upper spectrum in Figure 2 is typical following incubation of wild type yeast in [1,2-^{13}C]-acetate for 120 min. As we have previously observed (Trotter et al, 2005), the primary signals are from the five carbons of glutamate (labeled on the spectrum) and the carbons of sugars (at 60–95 ppm). As carbons of glutamate become ^{13}C-enriched, the singlet resonance(s) are split, due to the presence of the ^{13}C label at neighboring carbon(s), into characteristic multiplets (d, t and dd; expanded above the top spectrum for the five carbons of glutamate). The lower spectrum in Figure 2 was obtained from *gdh1* yeast in [1,2-^{13}C]-acetate for 120 min. Note that the vertical scale for *gdh1* spectrum has been magnified 7-fold. Thus, glutamate carbons labeled by [1,2-^{13}C]-acetate are easily observed in wild type cells; however, incorporation in *gdh1* is minimal, making detection and analysis of labeled glutamate carbons unfeasible in this strain.

Spectra similar to that in Figure 2 were generated from YNAceRaf-grown cells incubated in minimal medium with [1,2-^{13}C]-acetate for 0, 1 or 2 hours. NADP-GDH and the NAD-GDH activities measured under these conditions showed strain to strain comparisons as reported in Table 2 and no significant change in the activities during labeling period (data not shown). ^{13}C-Enrichment of C2 and C4 of glutamate was determined by integrating the total area under the curve for each signal and the ratio of enrichment at C2 and C4 was calculated. The data in Figure 3 demonstrate that over the time course, either the *gdh2Δ* or the *gdh3Δ* allele decreases the rate of C2 to C4 enrichment as compared to wild type. Additionally, the rate in the *gdh3Δ* strain is noticeably impaired as compared to the *gdh2Δ* strain.

As carbons in glutamate become increasingly ^{13}C-enriched, the peak patterns for each carbon become more complex. Generally, the complexity of the resonance pattern, that is the areas of multiplet resonances as compared to the area of the singlet peak, increases with time and/or with the number of times the carbon backbone is cycled before the α-ketoglutarate leaves the citric acid cycle for synthesis to glutamate (Jeffrey et al, 1991; Trotter et al, 2005; Turcotte et al, 2010). Alternatively, this parameter could be altered by entry of unlabeled, anaplerotic α-ketoglutarate derived from other cellular pools. An example of peak patterns at different times of enrichment in the *gdh2Δ* strain is shown in Figure 4A; the increase in complexity over time is most evident for C2 and C3. The intensities of multiplet (d, t, dd) and singlet peaks for C2, C3 and C4 for the wild type, *gdh2Δ* and *gdh3Δ* strains were integrated and calculated as a ratio of multiplet to singlet and are shown in Figure 4B. Data for carbons 1 and 5 are not included, since the intensity was weak and primarily multiplet (data not shown). The data show comparable ratios for wild type and *gdh2Δ* for nearly all the data points. The decreased complexity observed for *gdh2Δ*

and *gdh3Δ* at C2 may reflect the decreased rate of enrichment (Figure 2). So, despite the slower enrichment observed in *gdh2Δ* cells (Figure 3), the isotopomers formed in wild type and *gdh2Δ* cells are qualitatively similar. In contrast, the relative proportion of multiplet for C3 in the *gdh3Δ* strain, particularly at early time points, is noticeably elevated as compared to wild type and *gdh2Δ*. This trend is also seen at C4, but was not statistically significant (p values between 0.07 and 0.15). Since the enrichment of C2 compared to C4 is slower in these cells, these data suggest that the elevated isotopomer complexity reflects greater cycling of the backbone before conversion to glutamate.

Discussion

Saccharomyces cerevisiae expresses three glutamate dehydrogenases, each considered to have a particular function in glutamate metabolism under specific conditions. The Gdh1p and Gdh3p are primarily involved in glutamate biosynthesis, while Gdh2p is involved in glutamate degradation to ammonia and α-ketoglutarate (Magasanik, 2003). Gdh1p is active in cells grown on glucose as well as non-fermentable carbon sources, while Gdh3p is most active under non-fermentative or respiratory conditions (DeLuna et al, 2001; Riego et al, 2002; Avendano et al, 2005). Gdh2p is also elevated when cells are grown in low glucose or non-fermentable carbon (Coschigano et al, 1991). In the present study, we set out to examine these role(s) *in vivo* using stable isotope metabolic enrichment with [1,2-^{13}C]-acetate in single disruption mutants under conditions in which all three enzymes are active. To that end, we chose a mixture of acetate and the de-repressing sugar raffinose.

G*dh1Δ* cells are reported to have impaired growth on minimal glucose and ethanol media, indicating Gdh1p's importance to fermentative as well as respiratory growth (DeLuna et al, 2001; Magasanik, 2003). We did not observe any difference in doubling time for *gdh1Δ* cells as compared to wild type in our glucose medium (YNDex), which also contains 0.5% yeast extract. However, our *gdh1Δ* strain showed an impairment on minimal glucose medium similar to that reported (DeLuna et al, 2001; data not shown) and was unable to divide in the acetate/raffinose medium (Table 1). So, even though the relative proportion of Gdh3p activity increases in acetate/raffinose (Table 2), it is apparently insufficient to permit normal growth and glutamate synthesis without Gdh1p. ^{13}C-Enrichment experiments in *gdh1Δ* incubated in acetate/raffinose confirmed (Figure 2) that the Gdh1p enzyme is an important contributor to glutamate synthesis under these conditions.

Gdh3p is also required for normal growth on minimal ethanol medium, since *gdh3Δ* cells exhibit a doubling time of 67% as compared to wild type on this carbon source (DeLuna et al, 2001). Ethanol is converted to acetate for utilization as an energy and carbon source (Turcotte et al, 2010). Interestingly, we did not observe any defect for *gdh3Δ* cells on acetate/raffinose medium (Table 1), presumably because raffinose and 0.5% yeast extract were also in the medium. Yet, despite the wild type growth on acetate/raffinose medium, our ^{13}C-enrichment experiments demonstrate an important role for Gdh3p in glutamate metabolism from citric acid cycle intermediates under these conditions. First, the marked decrease in the rate of enrichment at C2 relative to C4 of glutamate observed in *gdh3Δ* (Figure 3) suggests a decrease in the flux of acetate carbons into the citric acid cycle. It has been reported that the pool of α-ketoglutarate in *gdh3Δ* cells grown on ethanol is 50% of that in wild type cells (DeLuna et al, 2001). So, the decreased rate of enrichment we observe may reflect a lower availability of α-ketoglutarate in *gdh3Δ* cells grown on acetate/raffinose.

The relative proportion of ^{13}C-label intensity observed in multiplet resonances as compared to singlet, particularly at C3 and C4, was greater in *gdh3Δ* cells as compared to wild type (Figure 4B). One interpretation of these data is that, before conversion to glutamate, the carbon backbones take a greater number of turns around the citric acid cycle, thereby

increasing the chances that neighboring carbons are ^{13}C labeled (Figure 1). If the *gdh3Δ* disruption does decrease the availability of α-ketoglutarate, it may be that the intermediate is conserved longer for use in turns of the citric acid cycle. Alternatively, these data may reflect a fundamental difference in the pool of glutamate synthesized by Gdh3p as compared to Gdh1p. Indeed, there is recent evidence that these enzymes have differential localization in the cell. Gdh3p was identified as a member of the mitochondrial proteome, while Gdh1p was not (Sickmann et al, 2003). So, the Gdh3p enzyme may have a unique relationship to α-ketoglutarate formed in the citric acid cycle. Taken together, the ^{13}C-enrichment data support an important role for Gdh3p in glutamate biosynthesis under de-repressing conditions.

Gdh2p, which serves primarily to convert glutamate back to α-ketoglutarate and ammonia (Magasanik, 2003), is greatly elevated in cells grown in acetate/raffinose (Table 2). Thus, although no growth defect was observed (Table 1), we anticipated that the *gdh2Δ* disruption might significantly alter glutamate homeostasis. The rate of ^{13}C-enrichment at C2 as compared to C4 was noticeably slower than wild type, but not as slow as was observed in the *gdh3Δ* cells (Figure 3). This indicates that the movement of the acetate label from the citric acid cycle to the glutamate pool is decreased in these cells. At first glance this result seems counterintuitive, since the Gdh2p is generally thought to be anaplerotic to the citric acid cycle, replenishing α-ketoglutarate levels as needed. Thus, loss of the enzyme might be expected to shift the pathway toward more glutamate biosynthesis, not less. However, this result may also reflect a slower flux through the cycle because the enzyme is not present to provide α-ketoglutarate. Unexpectedly, the ^{13}C-multiplet versus singlet pattern in the *gdh2Δ* cells was very similar to wild type. So, loss of Gdh2p does not seem to significantly alter the glutamate pool formed via this pathway.

It is interesting that despite the clear regulation of Gdh2p activity by carbon source, others have also had difficulty establishing a role for this enzyme in carbon metabolism (Coschigano et al, 1991). In fact, *gdh2Δ* cells do not display any growth impairment in media containing glucose or a non-fermentable carbon source and ammonia as the nitrogen source (Miller and Magasanik, 1990; Coschigano et al, 1991). It is important to note that acetate/raffinose medium used in our studies resulted in a ~20-fold increase in NAD-dependent activity as compared to glucose (Table 2), which is in line with the reported carbon source regulation of the *GDH2* gene (Coschigano et al, 1991). Levels of the Gdh2p enzyme are also separately regulated by the nitrogen source, generally being lower when ammonia or glutamine is the nitrogen source and higher when nitrogen is provided as glutamate or some other amino acids (Miller and Magasanik, 1990; Coschigano et al, 1991; Miller and Magasanik, 1991). Further, *gdh2Δ* cell growth is impaired as compared to wild type when nitrogen is provided exclusively as glutamate (Miller and Magasanik, 1990). Ammonia, rather than glutamate, was used as the nitrogen source for the present studies, so as to maximize ^{13}C-enrichment of the intracellular glutamate pool. It remains a possibility that the role of Gdh2p in glutamate metabolism might be more evident when a different nitrogen source is utilized and this is an area for future investigation.

Previous studies examining regulation of expression, as well as growth and levels of metabolic intermediates in mutants have indicated specific roles for these glutamate dehydrogenase isozymes (Magasanik, 2003; DeLuna et al, 2001; Coschigano et al, 1991; Miller and Magasanik, 1991). The present ^{13}C-enrichment study furthers the previous investigations by providing the first *in vivo* analysis of glutamate biosynthesis during aerobic metabolism in strains carrying disruptions in genes encoding these enzymes. The data confirm a primary role for Gdh1p in glutamate biosynthesis from citric acid cycle substrates. Additionally, loss of Gdh3p results in a significant impairment of glutamate synthesis, indicating an important role for this enzyme as well. Finally, loss of Gdh2p was

less deleterious to glutamate homeostasis than expected; however, further investigation under conditions in which Gdh2p activity is maximal may provide additional insight.

Acknowledgments

The authors thank Dr. Dennis Voelker (National Jewish Center, Denver) for sharing yeast strains and Mr. Evan Stoner for technical assistance. This work was supported by NIH grant R15-GM069372 (to P.J.T.) and by NSF Grant MRI/RUI CHE-0320267 (to P.J.T., Dr. Dick Narske and Dr. Dell Jensen).

References

Avendano A, Riego L, DeLuna A, Aranda C, Romero G, Ishida C, Vazquez-Acevedo M, Rodarte B, Recillas-Targa F, Valenzuela L, Zonszein S, Gonzalez A. Swi/SNF-GCN5-dependent chromatin remodelling determines induced expression of *GDH3*, one of the paralogous genes responsible for ammonium assimilation and glutamate biosynthesis in *Saccharomyces cerevisiae*. Mol Microbiol. 2005; 57(1):291–305. [PubMed: 15948967]

Burgess SC, Babcock EE, Jeffrey FMH, Sherry AD, Malloy CR. NMR indirect detection of glutamate to measure citric acid cycle flux in the isolated perfused rat heart. FEBS Lett. 2001:505163–167.

Coschigano PW, Miller SM, Magasanik B. Physiological and genetic analysis of the carbon regulation of the NAD-dependent glutamate dehydrogenase of *Saccharomyces cerevisiae*. Mol Cell Biol. 1991; 11(9):4455–4465. [PubMed: 1652057]

De Virgilio C, Burckert N, Barth G, Neuhaus JM, Boller T, Wiemken A. Cloning and disruption of a gene required for growth on acetate but not on ethanol: the acetyl-coenzyme A synthetase gene of *Saccharomyces cerevisiae*. Yeast. 1992; 8(12):1043–1051. [PubMed: 1363452]

DeLuna A, Avendano A, Riego L, Gonzalez A. NADP-Glutamate dehydrogenase isozymes of *Saccharomyces cerevisiae*. J Biol Chem. 2001; 276(47):43775–43783. [PubMed: 11562373]

Doherty D. L-Glutamate dehydrogenase in yeast. Meth Enzymol. 1970:17850–856.

Jeffrey FMH, Rajagopal A, Malloy CR, Sherry AD. 13C-NMR: a simple yet comprehensive method for analysis of intermediary metabolism. Trends Biochem Sci. 1991:165–10. [PubMed: 1909060]

Magasanik B. Ammonia assimilation by *Saccharomyces cerevisiae*. Eukaryot Cell. 2003; 2(5):827–829. [PubMed: 14555464]

Miller SM, Magasanik B. Role of the complex upstream region of the *GDH2* gene in nitrogen regulation of the NAD-linked glutamate dehydrogenase in *Saccharomyces cerevisiae*. Mol Cell Biol. 1991; 11(12):6229–6247. [PubMed: 1682801]

Miller SM, Magasanik B. Role of NAD-linked glutamate dehydrogenase in nitrogen metabolism in *Saccharomyces cerevisiae*. J Bacteriol. 1990; 172(9):4927–4935. [PubMed: 1975578]

Reilly C, Sherman R. Glucose repression of cytochrome A-synthesis in cytochrome-deficient mutants of yeast. Biochim Biophys Acta. 1965:95640–651.

Riego L, Avendano A, DeLuna A, Rodriguez E, Gonzalez A. *GDH1* expression is regulated by *GLN3*, *GCN4*, and *HAP4* under respiratory growth. Biochem Biophys Res Commun. 2002; 293(1):79–85. [PubMed: 12054566]

Sherman F. Getting started with yeast. Meth Enzymol. 1991:1943–21.

Sickmann A, Reinders J, Wagner Y, Joppich C, Zahedi R, Meyer HE, Schonfisch B, Perschil I, Chacinska A, Guiard B, Rehling P, Pfanner N, Meisinger C. The proteome of *Saccharomyces cerevisiae* mitochondria. Proc. Natl. Acad Sci USA. 2003; 100(23):13207–13212. [PubMed: 14576278]

Tenreiro S, Rosa PC, Viegas CA, Sa-Correia I. Expression of the *AZR1* gene (ORF YGR224w), encoding a plasma membrane transporter of the major facilitator superfamily, is required for adaptation to acetic acid and resistance to azoles in *Saccharomyces cerevisiae*. Yeast. 2000; 16(16):1469–1481. [PubMed: 11113970]

Trotter PJ, Adamson AL, Ghrist AC, Rowe L, Scott LR, Sherman MP, Stites NC, Sun Y, Tawiah-Boateng MA, Tibbetts AS, Wadington MC, West AC. Mitochondrial transporters involved in oleic acid utilization and glutamate metabolism in yeast. Arch Biochem Biophys. 2005; 442(1):21–32. [PubMed: 16140254]

Turcotte B, Liang XB, Robert F, Soontorngun N. Transcriptional regulation of nonfermentable carbon utilization in budding yeast. FEMS Yeast Res. 2010; 10(1):2–13. [PubMed: 19686338]

van den Berg MA, de Jong-Gubbels P, Kortland CJ, van Dijken JP, Pronk JT, Steensma HY. The two acetyl-coenzyme A synthetases of *Saccharomyces cerevisiae* differ with respect to kinetic properties and transcriptional regulation. J Biol Chem. 1996; 271(46):28953–28959. [PubMed: 8910545]

Zitomer RS, Nichols DL. Kinetics of glucose repression of yeast cytochrome c. J Bacteriol. 1978; 135(1):39–44. [PubMed: 209012]

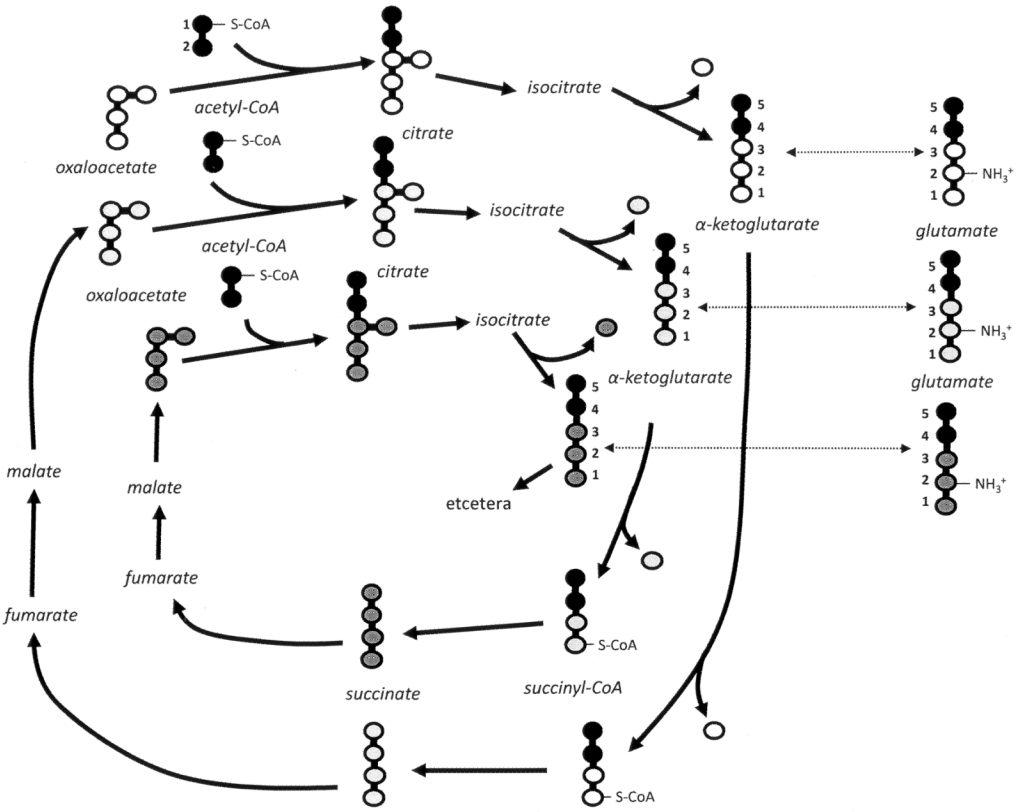

Figure 1.

Schematic depicting [1,2-^{13}C]-acetate incorporation, forming ^{13}C-isotopomers of glutamate with consecutive rotations of the citric acid cycle. Increasing enrichment of ^{13}C relative to ^{12}C is represented by darker shading.

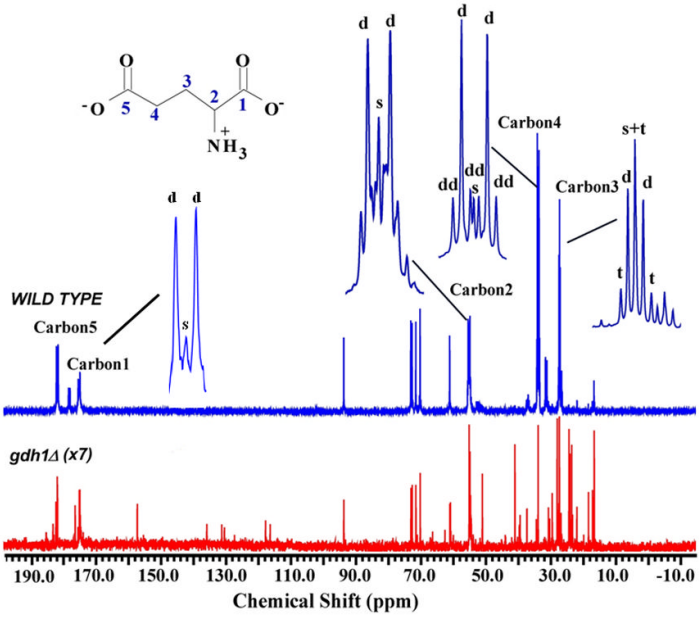

Figure 2.

Typical proton-decoupled ^{13}C-spectra for wild type (upper panel) and *gdh1Δ* (lower panel) strains after 2 hours in [1, 2-^{13}C]-acetate. Characteristic splitting of the singlet resonance(s) for glutamate carbons, due to the presence of the ^{13}C label at neighboring carbon(s), are expanded at the top (s, singlet; d, doublet, dd, doublet of doublet; t, triplet). Note that the *gdh1* spectrum has been magnified 7-fold.

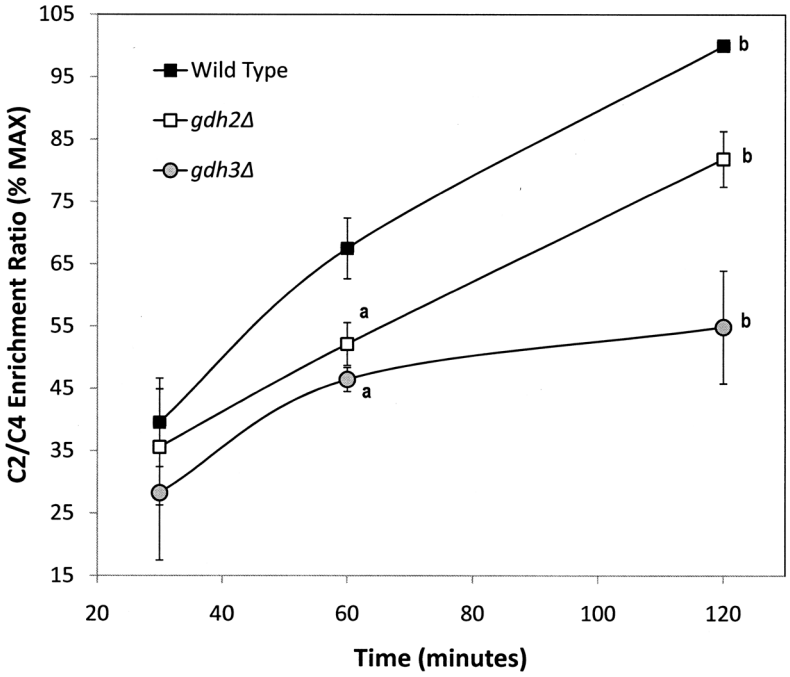

Figure 3.

The ratio of ^{13}C signal in carbon 2 relative to carbon 4 of glutamate during incorporation of [1,2-^{13}C]-acetate. The signal intensity, determined by integration, for carbon 2 was divided by that for carbon 4 (C2/C4 ratio). Data presented are the % of the maximal ratio (obtained for wild type at 120 minutes) +/− SEM from three separate experiments. a, $p < 0.05$ as compared to wild type at the same time point. b, $p < 0.05$ as compared to other strains at the same time point.

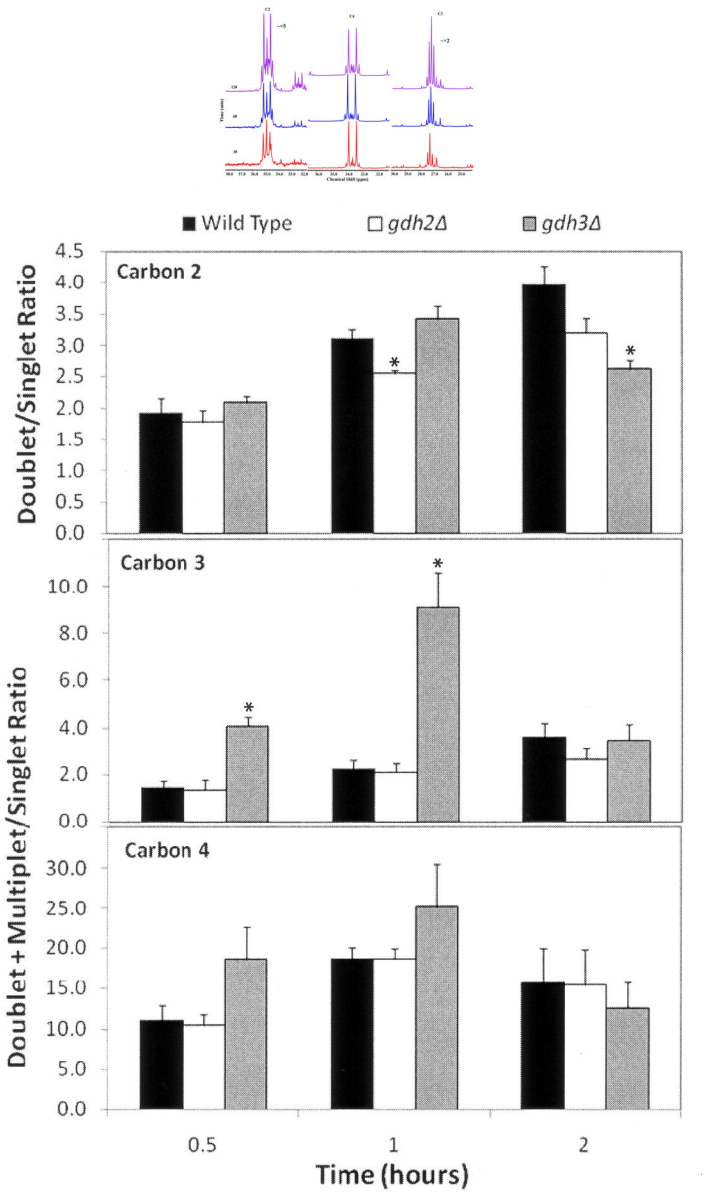

Figure 4.

Analysis of glutamate carbon ^{13}C signal complexity as a function of time in [1,2-^{13}C]-acetate. **(A)** Example of expanded spectra for carbons 2, 4, and 3 (C2, C4, and C3) from the *gdh2Δ* strain at 30, 60 and 120 minutes. **(B)** Intensity of multiplet resonances (d, t, dd) as compared to the singlet peak as a function of time. The intensities of multiplet and singlet peaks from three separate experiments were integrated and calculated as a ratio of multiplet to singlet +/− SEM. Data for carbons 1 and 5 are not included, since the intensity was weak and primarily multiplet (data not shown). *, $p < 0.05$ as compared to the other two strains for this carbon at the same time point.

Table 1

Strains and doubling times on experimental media

Strain[a]	Genotype	Doubling Time (minutes)[b]	
		YNDex	YNAceRaf
Wild Type (BY4742)	*MATα his3 leu2 lys2 ura3*	127+13	254+43
gdh1Δ (*YOR375c*)	*MATα his3 leu2 lys2 ura3 gdh1Δ::G418*	132+11	ND[c]
gdh2Δ (*YDL215c*)	*MATα his3 leu2 lys2 ura3 gdh2Δ::G418*	132+6	232+43
gdh3Δ (*YAL062w*)	*MATα his3 leu2 lys2 ura3 gdh3Δ::G418*	133+6	272+33

[a] Wild type is followed in parentheses by the strain name; for mutants the strain name used in these studies is followed in parentheses by the designation for the disrupted open reading frame.

[b] Doubling times during logarithmic growth in glucose (YNDex) or acetate plus raffinose media (YNAceRaf); Average of 3–5 separate determinations +/− standard deviation. ND = not detectable

[c] Although the *gdh1Δ* strain does not divide, no loss of viability is observed after 17–19 hours in this medium.

Table 2

Glutamate dehydrogenase activities in strains grown on experimental media

Strain	NADP-GDH Activity (μmol/min/mg)[a]		NAD-GDH Activity (μmol/min/mg)[b]	
	YNDex	YNAceRaf	YNDex	YNAceRaf
Wild Type	154+26	24+6[c]	6.2+4.3	108+13[c]
gdh1Δ	1.0+0.4	3.2+1.1[d]	5.8+6.3	14+2[d, e]
gdh2Δ	154+10	24+6[c]	1.8+0.2	1.2+0.3
gdh3Δ	125+15	21+6[c]	2.9+0.3	85+9[c]

[a] NADP-dependent measures Gdh1p and Gdh3p activity. Data are the average +/− standard error for 4 or 5 separate determinations.

[b] NAD-dependent measures Gdh2p activity. Data are the average +/− standard error for 2 or 3 (YNDex) or 5 (YNAceRaf) separate determinations.

[c] $p < 0.001$ by t-test as compared to activity of the same strain in glucose.

[d] $p < 0.08$ by t-test as compared to activity of the same strain in glucose.

[e] $p < 0.001$ by t-test as compared to activity of wild type or *gdh3Δ* in YNAceRaf.